System identification algorithms for the analysis of dielectric responses from broadband spectroscopies

System identification algorithms for the analysis of dielectric responses from broadband spectroscopies

2011 J. Phys.: Conf. Ser. 310 012002

(http://iopscience.iop.org/1742-6596/310/1/012002)

System identification algorithms for the analysis of dielectric responses from broadband spectroscopies

S. Hadjiloucas[1], G.C. Walker[1], J.W. Bowen[1], and R.K.H. Galvão[2]

[1]Cybernetics, School of Systems Engineering, The University of Reading, RG6 6AY, UK

[2]Divisão de Engenharia Eletrônica, Instituto Tecnológico de Aeronáutica, São José dos Campos, SP, 12228-900 Brazil.

Email: s.hadjiloucas@reading.ac.uk

Abstract. We discuss the modelling of dielectric responses for an electromagnetically excited network of capacitors and resistors using a systems identification framework. Standard models that assume integral order dynamics are augmented to incorporate fractional order dynamics. This enables us to relate more faithfully the modelled responses to those reported in the Dielectrics literature.

1. Introduction

Over the past several years, our group has been building Fourier transform spectrometers for the far-infrared part of the spectrum and as a consequence, we have developed signal processing algorithms for de-noising and classification by decomposing the signals in the Fourier, windowed-Fourier, principal component and wavelet domains [1-3]. Furthermore, we have adopted a systems identification framework [4-7] for the direct analysis of signals in the time domain, obviating the commonly used ratioing procedure to evaluate the sample's insertion loss. Our modeling approach has been only valid, however, when the dispersive phenomena are governed by de-embeddable Lorentzian, Debye and Drude responses.

In addition, a significant body of literature has come to our attention, where the dielectric responses (frequency dependent permittivity and AC conductivity) of heterogeneous materials such as glasses, ceramics, amorphous semiconductors, heavily doped crystals, polymers, and composites can be modeled under the assumption that they behave as micro-structured electrical networks containing capacitive (insulating) and resistive (conducting) regions [8-18]. Often, the experimentally observed AC conductivity $\sigma(\omega)$ follows a Jonscher [19, 20] power law $\sigma(\omega)=\sigma(0)+A\omega^q$ where ω is the excitation angular frequency, $\sigma(0)$ is the DC conductivity, A is a proportionality constant and $0.5<q<0.7$. From this power law, as $\omega\to\infty$, the well-known irrational Cole-Davidson formula for complex permittivity is obtained:

$$\varepsilon^* \approx \frac{1}{(1+i\omega\tau)^{(1-q)}} \tag{1}$$

Since in the Laplace domain, the above expression is not of integral order, we propose the use of fractional order models [21] to describe such processes. The Riemann-Liouville definition of fractional integral and corresponding fractional order derivative is adopted to solve the corresponding fractional order differential equations of the underlying system dynamics:

$$ {}_0d_t^{-q} f(t) = \frac{1}{\Gamma(q)} \int_0^t (t-\tau)^{q-1} f(\tau) d\tau, \quad q \geq 0 \tag{2a} $$

$$ {}_0d_t^{p} f(t) = \frac{1}{\Gamma(1-p)} \int_0^t (t-\tau)^{-p} f(\tau) d\tau, \quad 0 < p < 1 \tag{2b} $$

where $\Gamma(q)$ denotes the Euler gamma function.

2. Signal processing schemes within a fractional order identification framework

The dynamics of an unknown medium may be modeled using an input-output state space representation and a subspace multiple input-multiple output (MIMO) model may be fitted [21]. The fractional state space representation for the system is given from:

$$ D^a \mathbf{x}(t) = A\mathbf{x}(t) + B\mathbf{u}(t) \tag{3a} $$

$$ \mathbf{y}(t) = C\mathbf{x}(t) + D\mathbf{u}(t) \tag{3b} $$

where $\mathbf{x} \in \mathbb{R}^n$ is the state vector, $\mathbf{u} \in \mathbb{R}^m$ is the input vector, $\mathbf{y} \in \mathbb{R}^p$ is the output vector and $A \in \mathbb{R}^{n \times n}$, $B \in \mathbb{R}^{n \times m}$, $C \in \mathbb{R}^{p \times n}$ and $D \in \mathbb{R}^{p \times m}$ are the state, input, output and feed-through system constant matrices to be determined. As discussed in [22], such fractional order system is stable if $0 < \alpha < 2$ and $\left|\arg(\lambda_k)\right| > \alpha\pi / 2$ and $-\pi < \arg(\lambda_k) \leq \pi$ where λ_k corresponds to the k^{th} eigenvalue of A. For time-domain simulations of a system, a recursive distribution of poles and zeros is obtained to approximate the frequency behavior of s^a over an interval $[\omega_A, \omega_B]$. Because the asymptotic behavior at the low and high limits of the above frequency interval can have a static error between the fractional order model and its approximation, it is common to minimize this using an integrator operating outside that interval.

Given a large number of inputs and outputs related to the unknown dielectric system, the goal of the subspace algorithms is to determine the order of the system, A, B, C, D (to a similarity transformation). For simplicity, we are only considering the deterministic case where there is no noise in the measured inputs or process (estimated state) although the proposed approach is also valid to the stochastic case where an explicit augmented model in innovation form can be considered. In that case, an additional step is required to obtain an estimate of covariance matrices of the noise sequences.

A linear order model is obtained after computing the successive α-order fractional derivatives of (3). After substitution, an extended linear model $\bar{\mathbf{y}}(t) = \Gamma_i^* \mathbf{x}(t) + \Delta_i^* \bar{\mathbf{u}}(t)$ is obtained with input and output variables:

$$ \bar{\mathbf{u}}(t) = \left[\mathbf{u}(t)^T \quad D^\alpha \mathbf{u}(t)^T \quad \ldots \quad D^{i\alpha} \mathbf{u}(t)^T \right]^T \tag{4a} $$

$$ \bar{\mathbf{y}}(t) = \left[\mathbf{y}(t)^T \quad D^\alpha \mathbf{y}(t)^T \quad \ldots \quad D^{i\alpha} \mathbf{y}(t)^T \right]^T \tag{4b} $$

where

$$ \Gamma_i^* = \left[C \quad CA \quad \cdots \quad CA^{i-1} \right]^T \in \mathbb{R}^{ip \times n} \tag{5a} $$

$$ \Delta_i^* = \begin{bmatrix} D & 0 & \cdots & 0 \\ CB & D & \ddots & \vdots \\ \vdots & \ddots & \ddots & 0 \\ CA^{i-2}B & \cdots & CB & D \end{bmatrix} \in \mathbb{R}^{ip \times im} \tag{5b} $$

correspond to the observability and controllability matrices.

Because a successive differentiation of the input-output data introduces additional noise from the high-pass filter action, a fractional order low-pass filter with corner frequency ω_f is introduced $F(s) = \left(1 + \tau s^\alpha\right)^{-1}$ where $\tau = \left(\omega_f\right)^{-\alpha}$ to provide numerical stability. This filter multiplies the Laplace transform of (3) and the result is inverse Laplace transformed to the time domain to obtain:

$$ \mathbf{x}(t) = A_F \left[\lambda \mathbf{x}(t) \right] + B_F \left[\lambda \mathbf{u}(t) \right] \tag{6a} $$

$$ \mathbf{y}(t) = C\mathbf{x}(t) + D\mathbf{u}(t) \tag{6b} $$

where $A_F = I + \tau A$, $B_F = \tau B$ and $\lambda = \Im^{-1}\left(F(s)\right)$ with $\Im$ denoting the Laplace operator and I the identity matrix. Using recursion on expression (6b), new filtered input and output vectors are constructed as well as observability and controllability matrices:

$$\mathbf{U}(t) = \left[\lambda^{i-1}\mathbf{u}(t) \quad \lambda^{i-2}\mathbf{u}(t) \quad \dots \quad \mathbf{u}(t)\right]^T \tag{7a}$$

$$\mathbf{Y}(t) = \left[\lambda^{i-1}\mathbf{y}(t) \quad \lambda^{i-2}\mathbf{y}(t) \quad \dots \quad \mathbf{y}(t)\right]^T \tag{7b}$$

$$\Gamma_i = \left[C \quad CA_F \quad \cdots \quad CA_F^{i-1}\right]^T \in \mathbb{R}^{ip\times n} \tag{7c}$$

$$\Delta_i = \begin{bmatrix} D & 0 & \cdots & 0 \\ CB_F & D & \ddots & \vdots \\ \vdots & \ddots & \ddots & 0 \\ CA^{i-2}B_F & \cdots & CB_F & D \end{bmatrix} \in \mathbb{R}^{ip\times im} \tag{7d}$$

The subsequent estimation of the A, B, C, D matrices follows the standard MOESP subspace identification routines discussed in the literature [23-27] by applying them to expressions 7a-7d. For brevity reasons these will not be further discussed here.

The fractional derivative order $\alpha \in (0,2)$ is considered unknown and is estimated by minimizing:

$$\hat{\alpha} = \underset{\alpha\in(0,2)}{\arg\min}\frac{1}{2}\left\|\hat{\mathbf{y}}_c(\alpha) - \mathbf{y}_c\right\|_2^2 \tag{8}$$

where $\mathbf{y}_c$ is the vector obtained by concatenating the system outputs and $\hat{\mathbf{y}}_c(\alpha)$ is the vector obtained by concatenating the outputs of the state-space representation estimated with the subspace model.

3. Modelling of dielectric responses

Figure 1 shows a generic dielectric network composed of resistors and capacitors connected in either series or parallel configurations.

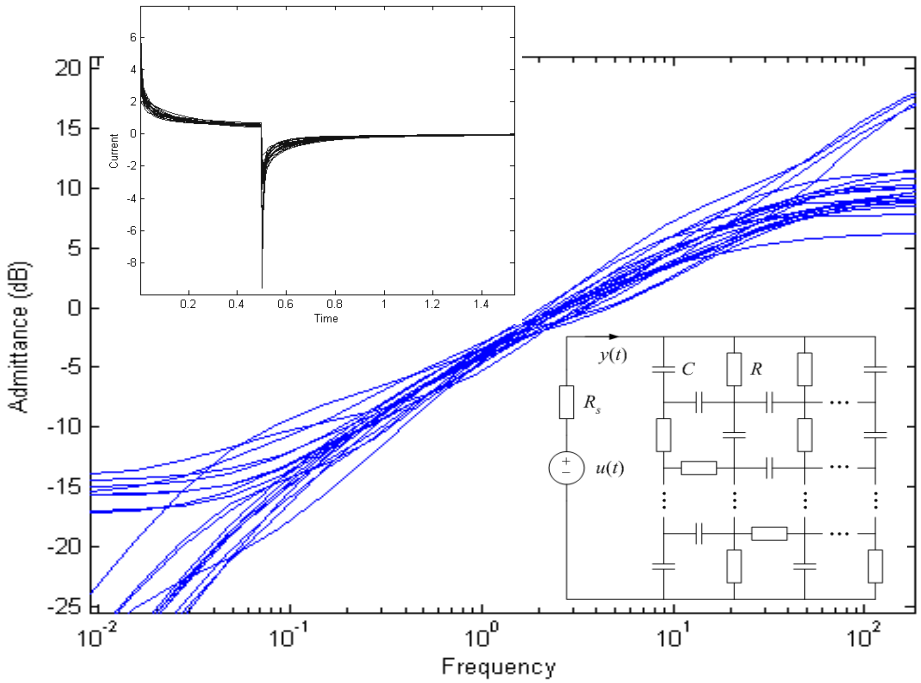

Figure 1. Simulated frequency response (admittance) of the dielectric network including the source resistance. Each line corresponds to one of the 20 random realizations assuming 5 hidden layers of nodes and 5 nodes per hidden layer. The insets shows the current pulse excitation and the random network of *R*, *C* components considered. The output resistance of the source is denoted by R_s.

The term "layer" will refer to a layer of nodes. The top and bottom layers are connected to the source. The intermediate layers are termed "hidden layers". The qualitative differences in the admittance responses can be ascribed to the position of the *R*, *C* components in the network. If there is any pure resistive path connecting the source with the ground, the low-frequency (DC) admittance will be different from zero. If there is no such path, the DC admittance will be zero (tending to minus infinity in dB). In the latter case, there is at least one capacitor blocking the DC current from the source to the ground. The presence/absence of pure resistive paths depends on the position of the components, which is chosen in a random manner. In the simulations performed, the elements have adopted values: $R_s = 0.1$, $R = 1$, $C = 0.5$ and different network realizations are considered.

The simulations always incorporate a resistor at the source output. Such a resistor can be used to model the output resistance of the source or the resistance of the interface between the source and the dielectric material. Moreover, the presence of such a resistor is important to eliminate inconsistencies in the model. For example, it makes no sense to connect the terminals of an ideal voltage source to a capacitor, as the capacitor voltage cannot undergo instantaneous changes. Following the work by Almond's group [10-14], the Matlab results presented here were further validated against those obtained by using the ORCAD 16.3 software to run SPICE simulations.

Figure 1 shows results obtained for 20 random networks (5 hidden layers of nodes, 5 nodes per hidden layer) in response to a rectangular pulse excitation $u(t)$ with duration 0.5 and unit amplitude. Figure 2 shows the time-domain current response of a particular network realization shown in the inset of figure 1 to a chirp excitation $u(t)$ with frequency ranging from 0 to 20 Hz and the corresponding N4SID models for integral order ranging from one to five.

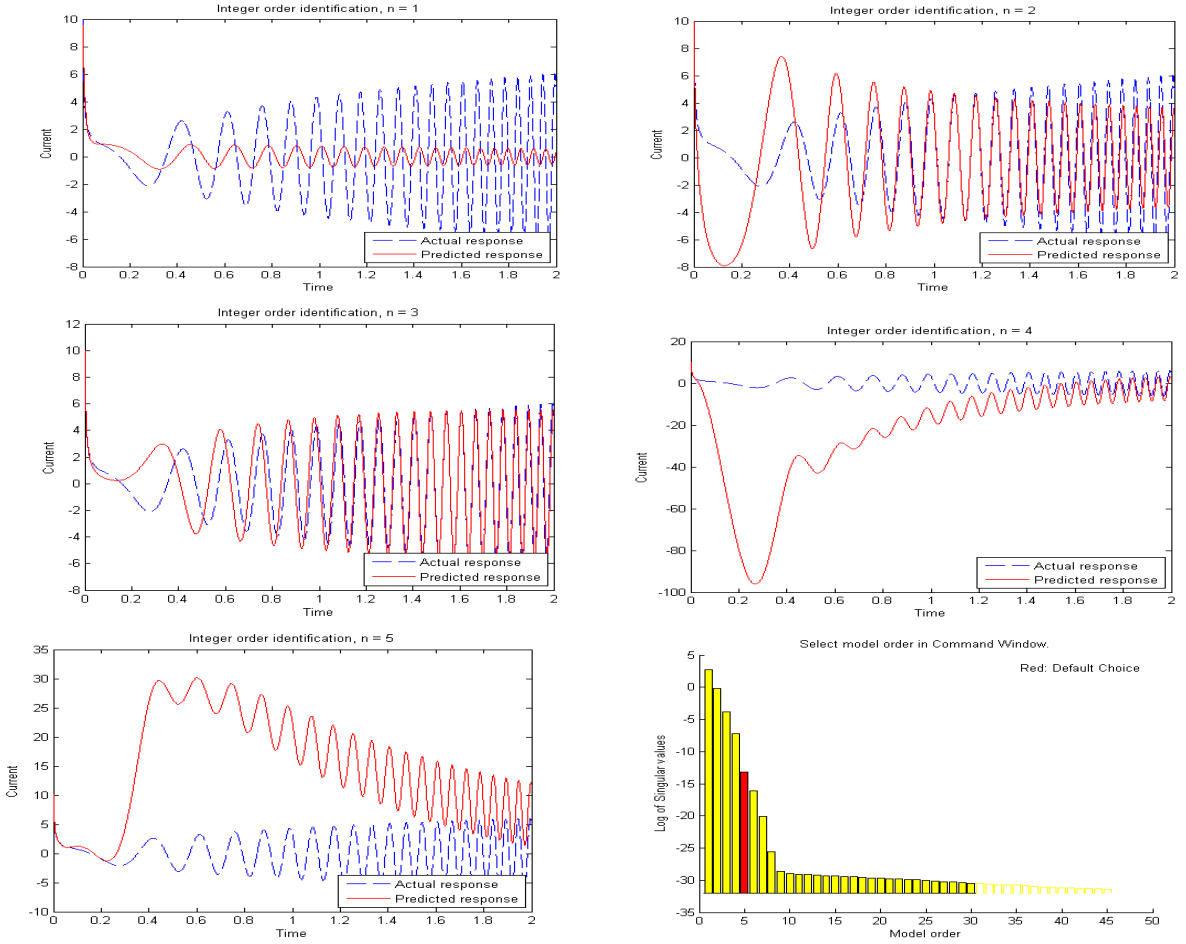

Figure 2. Current time domain response of a particular network to a chirp excitation $u(t)$ with frequency ranging from 0 to 20 Hz and N4SID models of integral orders *n* ranging from one to five.

These responses were obtained by stimulating the model dielectric with the same chirp input employed in the identification. In this case, the actual order of the input-output dynamics is 22. As can be seen, the difference between the actual and predicted responses decreases as the order is increased from one to three. However, the results become poor when the order is further increased, which may point to ill-

conditioning problems in the identification process. Integral order subspace algorithms may not capture faithfully the dynamics of the dielectric sample under consideration.

Figure 3 presents the response of a fractional-order model identified by using customized simulations with a fractional order subspace algorithm. In this case, the identification was initialized by using the first-order N4SID model. As can be seen, the agreement between actual and predicted responses is a considerable improvement on the results of the integer-order models presented in Figure 2.

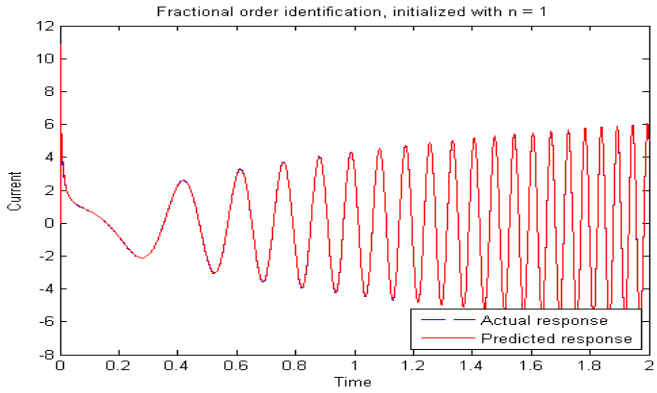

Figure 3. Time response of the identified fractional-order model.

A voltage-to-current transfer function $\left(0.098s^{0.88}+0.52s^{0.29}\right)\left(0.0096s^{0.91}+1\right)^{-1}$ for the identified fractional-order model was obtained for the particular realization used in the simulations (where the notation $s = j\omega$ implies that the transfer function is in the Laplace domain).

Figure 4 compares the frequency response of the best integer-order model (n = 3) and the fractional order model against the admittance of the actual circuit. As can be seen, the fractional-order model agrees with the expected response across a wider range of frequencies, which encompasses the spectral content of the chirp excitation employed in the identification procedure.

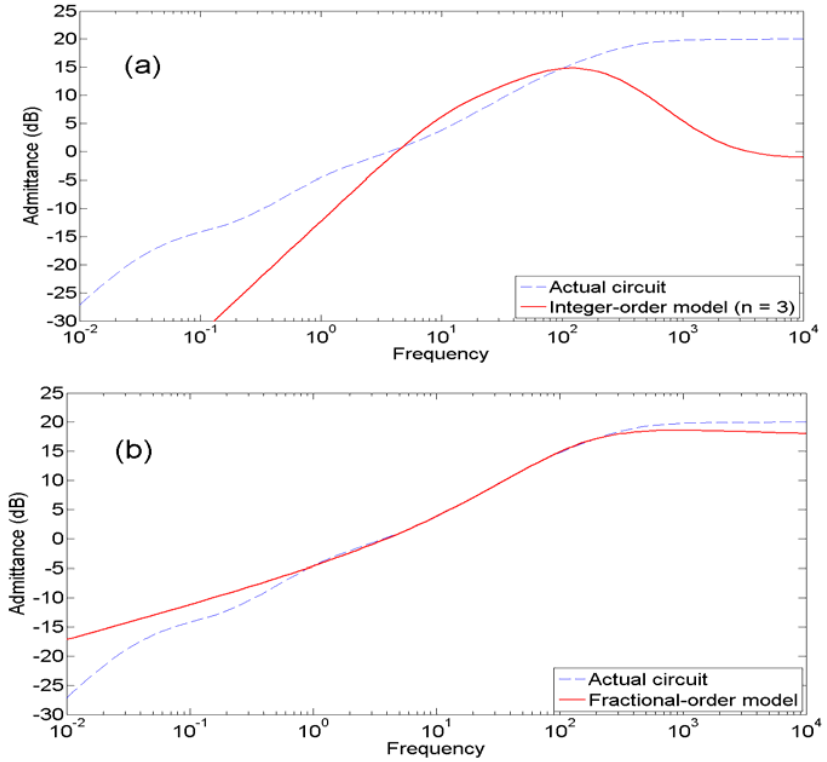

Figure 4. Frequency response of the identified models of (a) integer order n = 3 and (b) fractional order. Better matching between the actual circuit and the model response over 2 decades is obtained with the fractional order model.

4. Discussion

In the current framework, from an experimental perspective, we are assuming there are no additional artifacts from the propagation of the broadband excitation within the sample or from the process of gating the detector. It must be noted, however, that for the case of broadband excitation using a continuous wave Fourier transform spectrometer, where the sample is located in front of the detector after the two partial beams have recombined, there may be leakage of cross-polar components from the interaction of the sample with the beam [28] or pseudocoherence errors [29, 30] because different parts of the beam travel different paths through different regions of the sample (if this is of non-uniform thickness), interfering constructively or destructively with each other when they recombine. In addition, in the microwave and THz parts of the spectrum, in the case of continuous wave dispersive Fourier transform spectrometry, where the sample is located in one arm of the interferometer (here we are assuming a Michelson, Mach Zehnder or their polarization variance topologies) there could be some additional 'beam dilution' errors because the beam spreads diffractively at different rates along the axes of propagation in the reference and sample arms [31, 32]. This is further exacerbated in fast pulse spectroscopies where tight focusing of the IR beam is necessary unless an ASOPS detector interrogation scheme is utilized [8, 33]. Furthermore, in the case where a picosecond or femtosecond system has been used to electromagnetically excite the sample at the UV, optical, infrared, THz or microwave parts of the spectrum, there will be additional errors from the tight focusing of the beam to the sample or the detector and the beam may not be modeled under the assumption of plane wave incidence on the sample. Experimentally obtained dielectric responses often incorporate such artifacts and so the associated data-driven system identification models are expected to show deviations from theoretical responses. Interestingly, fractional order Fourier transforms can also be used to decompose the propagating EM beam modes inside the sample or in free space so the proposed formulation is also appropriate for the study of optical systems in general.

5. Conclusion

Jonscher's universal dielectric response of a random network of capacitors and resistors has been considered under a systems identification framework and a new approach using fractional order models is proposed. The scheme is particularly promising for modeling the responses of mixtures, where several species with different dielectric properties are present within the sample. It can also be used for de-noising purposes in a signal processing framework, as well as for sample classification purposes within a chemometric quality assurance context. Appropriate Matlab tools are currently under development to identify and validate fractional order models. The detailed mathematical formulation of fractional order identification tools and in particular the formulation of fractional order subspace models will be discussed at the conference.

References

[1] Galvão RKH, Hadjiloucas S, Bowen JW, and Coelho CJ, 2003 *Opt. Express*, **11**, 1462-1473.
[2] Hadjiloucas S, Galvão RKH and Bowen JW 2002 *J. Opt. Soc. Am. A* **19**, 2495-2509.
[3] Galvão, RKH, Hadjiloucas S, Zafiropoulos A, Walker GC, Bowen JW and Dudley R, 2007 *Opt. Lett.*, **32**, 3008-3010.
[4] Hadjiloucas S, Galvão RKH, Becerra VM, Bowen JW, Martini R, Brucherseifer M, Pellemans HPM, Haring Bolívar P, Kurz H, Chamberlain JM 2004 *IEEE Trans. Microw. Theory*, **52**, 2409-2419.
[5] Fischer BM, Yin X, Ng BW-H, Abbott D, Paiva HM, Galvão RKH, Hadjiloucas S, Walker GC, and Bowen JW, 2008 'Subspace and Wavelet-Packet Algorithms for de-noising and classifying broadband THz transients,' *Joint 33rd Int.Conf. Infrared and Millimetre Waves and 16th Int.Conf. Terahertz Electronics*, Caltech, USA.
[6] Yin X, Fischer BM, Ng BW-H, Abbott D, Paiva HM, Galvão RKH, Hadjiloucas S, Walker GC and Bowen JW 2007 In *Microelectronics: Design, Technology, and Packaging III*, (Eds. Alex J. Hariz, Vijay K. Varadan), Proc. SPIE **6798**, pp. 679814.
[7] Hadjiloucas S, Walker GC, Bowen JW, Becerra VM, Zafiropoulos A and Galvão RKH 2009 *J. Phys. Conf. Ser.*, **183** 012003
[8] Nowick AS, Vaysleyb AV and Kuskovsky I 1998 *Phys. Rev. B*, **58**, pp. 8398-8406.
[9] Panteny S, Stevens R and Bowen CR 2005 *Ferroelectrics*, **319**, pp. 199-208.
[10] Almond DP, Vainas B and Uvarov NF 1998 *Solid State Ionics*, **111**, pp. 253-261.
[11] Vainas B, Almond DP, Luo J and Stevens R 1999 *Solid State Ionics*, **126**, pp. 65-80.
[12] Almond DP, Bowen CR and Rees DAS 2006 *J. Phy. D. Appl. Phys.*, **39**, pp.1295-1304.

[13] Bouamrane R and Almond DP 2003 *J. Phys. Condens. Matt.*, **15**, pp. 4089-4100.
[14] McCullen NJ, Almond DP, Budd CJ and Hunt GW 2009 *J. Phys. D Appl. Phys.*, **42**, 064001.
[15] Dyre JC 1991 *J. Non-Crystal. Solids*, **135**, pp. 219-226.
[16] Wieczorek W, Zalewska A, Siekierski M and Przyluski J 1996 *Solid State Ionics*, **86-88**, pp. 357-362.
[17] Nowick AS and Lim BS 2001 *Phys. Rev. B*, **63**, 184115.
[18] Sidebottom DL 1999 *Phys. Rev. Lett.*, **83**, pp. 983-986.
[19] Jonscher AK 1977 'The universal dielectric response' *Nature* (London) 267, pp. 673-679.
[20] A.K. Jonscher AK *Dielectric Relaxation in Solids* (Chelsea Dielectrics Press, London, 1983).
[21] Hartley TT, Lorenzo CF, 2003 *Signal Process.*, **83**, pp. 2287-2300.
[22] Matignon D 1998 Stability properties for generalized fractinal differential systems, In *ESAIM: Proc. Fractional Differential Systems: Models, Methods and Applications*, **5**, 145-158.
[23] van Overschee P and De Moor B 1994 *Automatica* **30** 75–93
[24] Katayama T (2005), *Subspace methods for system identification*, Springer.
[25] Favoreel W, De Moor B, Van Overschee P 2000 *J. Process Contr.*, **10**, pp. 149-155.
[26] Viberg M, 1995, *Automatica*, **31**, 1835-1851.
[27] Galvão RKH, Hadjiloucas S, Becerra VM and Bowen JW 2005 *Meas. Sci. Technol.*, **16**, 1037-1053.
[28] Bowen JW, Walker GC and Hadjiloucas S. 2007 *Joint 32nd Int.Conf. Infrared and Millimetre Waves and 15th Int. Conf. Terahertz Electronics*, Cardiff, UK pp.208-209 IEEE Cat. number 07EX1863.
[29] Hadjiloucas S, Karatzas LS and Bowen JW 1999 *IEEE Trans. Microw. Theory*, **47**, 142-149.
[30] Walker 2003 GC '*Modelling the Propagation of Terahertz Radiation in Biological Tissue*' PhD Thesis, Centre of Medical Imaging Research, University of Leeds.
[31] Bowen JW, Walker GC, Hadjiloucas S and Berry EA 2004 'The consequences of diffractively spreading beams in ultrafast THz spectroscopy,' *Joint 29th International Conference on Infrared and Millimeter Waves and 12th International Conference on Terahertz Electronics*, Karlsruhe, Germany pp. 551-552, IEEE Catalog Number 04EX857.
[32] Walker GC, Bowen JW, Zafiropoulos A, Hadlington T, Hadjiloucas S, Chamberlain JM 2007 *Joint 32nd Int.Conf. Infrared and Millimetre Waves and 15th Int. Conf. Terahertz Electronics*, Cardiff, UK pp. 512-513. IEEE Cat. number 07EX1863.
[33] Bartels A, Cerna R, Kistner C, Thoma A, Hudert F, Janke C, and Dekorsy T 2007 *Rev. Sci. Instrum.* **78**, 035107.